Journal of Photochemistry and Photobiology B: Biology 122 (2013) 15–23

Contents lists available at SciVerse ScienceDirect

Journal of Photochemistry and Photobiology B: Biology

journal homepage: www.elsevier.com/locate/jphotobiol

Synthesis, characterization and DNA interaction of new copper(II) complexes of Schiff base-aroylhydrazones bearing naphthalene ring

Cansu Gökçe, Ramazan Gup *

Mugla Sıtkı Koçman University, Department of Chemistry, 48000 Mugla, Turkey

ARTICLE INFO

Article history:
Received 20 December 2012
Received in revised form 21 February 2013
Accepted 25 February 2013
Available online 14 March 2013

Keywords:
Aroylhydrazone
Naphthalene ring
Copper(II) complexes DNA binding
DNA cleavage

ABSTRACT

Two new copper(II) complexes with the condensation products of methyl 2-naphthyl ketone with 4-hydroxybenzohydrazide, 4-hydroxy-*N*′-[(1*Z*)-1-(naphthalen-2-yl)ethylidene]benzohydrazide [HL^1] and (Z)-ethyl 2-(4-(2-(1-(naphthalen-2-yl)ethylidene)hydrazinecarbonyl)phenoxy)acetate (HL^2) were synthesized and characterized by elemental analysis, infrared spectra, UV–Vis electronic absorption spectra, magnetic susceptibility measurements, TGA, powder XRD and SEM–EDS. The binding properties of the copper(II) complexes with calf thymus DNA were studied by using the absorption titration method. DNA cleavage activities of the synthesized copper complexes were examined by using agarose gel electrophoresis. The effect of complex concentration on the DNA cleavage reactions in the absence and presence of H_2O_2 was also investigated. The experimental results suggest that the copper complexes bind significantly to calf thymus DNA by both groove binding and intercalation modes and cleavage effectively pBR322 DNA. The mechanistic studies demonstrate that a hydrogen peroxide-derived species and singlet oxygen ($^1O_2$) are the active oxidative species for DNA cleavage.

1. Introduction

The interaction of coordination compounds with DNA has been of interest due to their possible applications in cancer therapy [1–5] and molecular biology [6,7]. They show unique spectral and electrochemical properties, as well as the ability of their ligands to be adjusted to DNA interaction abilities. Schiff base complexes have been attracted much attention due to their significances in the development of new therapeutic agents and novel nucleic acid structural probes [8–11]. Copper is an important trace element for plants and animals and is involved in complex formation in a number of biological processes [12–14]. Copper(II) complexes have found possible medical uses in the treatment of many diseases including cancer [15,16]. Therefore, investigations on copper complexes are becoming more prominent in the research area of bioinorganic chemistry [17–23]. Copper complexes have been known to cleave DNA by different mechanisms viz. hydrolytic [24] and oxidative pathways [25]. Artificial metallonucleases require ligands, delivering the metal ion to the proximity of DNA. Aroylhydrazone type ligands have a large number of potential donor atoms and hence display versatile behavior in metal coordination. The mode of coordination depends on the nature of the central metal atom, type of the ligand as well as on the presence of other species capable to compete for coordination pockets. Herein, we described the synthesis and characterization of new Cu(II) complexes of Schiff base-hydrazone ligands and their DNA binding and cleavage activities.

2. Experimental

2.1. Material

All chemicals used were analytical reagent grade. Copper(II) acetate, ethyl 4-hydroxybenzoate, methyl 2-naphthyl ketone, ethyl bromoacetate, K_2CO_3, acetone and hydrazine monohydrate were purchased from Fluka and Sigma–Aldrich and used without further purification. Calf thymus DNA (CT-DNA) was purchased from Sigma–Aldrich. pBR322 DNA was purchased from Fermantas. ^1H and ^{13}C NMR spectra were recorded on a Bruker 400 MHz spectrometer in DMSO_d_6 with TMS as the internal standard. IR spectra were recorded on a Perkin Elmer 1605 FTIR spectrometer as KBr pellets. The electronic spectra of the ligands and complexes were recorded on a UV-1601 Shimadzu spectrophotometer. Carbon, hydrogen and nitrogen analyses were carried out on a LECO 932 CHNS analyzer and copper content was determined by atomic absorption spectroscopy using the DV 2000 Perkin Elber ICP-AES. Room temperature magnetic susceptibility measurements were carried out on powdered samples using a Sherwood Scientific MK1 Model Gouy Magnetic Susceptibility Balance. Melting points were determined on an Electrothermal IA 9100 digital melting point apparatus. The thermogravimetric analysis was carried out in dynamic

* Corresponding author. Tel.: +90 2522111496; fax: +90 2522111472.
E-mail address: rgup@mu.edu.tr (R. Gup).

1011-1344/$ - see front matter © 2013 Elsevier B.V. All rights reserved.
http://dx.doi.org/10.1016/j.jphotobiol.2013.02.014

nitrogen atmosphere (20 mL min^{-1}) with a heating rate of 20 °C min^{-1} using a Perkin Elmer Pyris 1 TGA thermal analyzer in the Central Laboratory at METU. SEM investigations were performed using a JEOL SEM 7700F, equipped with an EDS system in the Central Laboratory at Mugla Sıtkı Koçman University. The XRD analyses of the powder samples were recorded with a Rigaku Corporation X-ray diffractometer (Model smartlab) analyzer in the Central Laboratory at Mugla Sıtkı Koçman University. All the diffraction patterns were obtained by using Cu $K\alpha_1$ radiation, with a graphite monochromator at 5j/min scanning rate. The Schiff base-hydrazone ligands were prepared according to Scheme 1.

2.2. Synthesis of 4-hydroxy-N′-[(1Z)-1-(naphthalen-2-yl) ethylidene]benzohydrazide (HL^1)

Methyl 2-naphthyl ketone (1 mmol, 0.170 g) dissolved in ethanol (10 mL) was added drop wise to a suspension of 4-hydroxybenzohydrazide (I) (4 mmol, 0.152 g) with two drops of glacial acetic acid in ethanol (15 mL) in room temperature. The reaction mixture was refluxed for further 8 h and the colorless product was filtered. The pure aroylhydrazone was collected by crystallization from acetone.

Yield 77%; Mp 249–251 °C; UV (EtOH, nm) 267, 302, 389; IR (KBr) (ν, cm^{-1}) 3290 (OH), 1634 $(C{=}O)_{amide}$, 1606 (C═N), 1371 (C—N), 1234 and 1175 (C—O—C); ^1H NMR (DMSO_d_6, ppm) δ 2.48 (s, 3H, N═C—CH_3), 6.89 (d, 2H, J = 8.3, ArH^d), 7.52 (d, 2H, J = 8.3, ArH^e), 7.83–8–29 (m, 7H, ArH), 10.15 (s, 1H, OH), 10.64 (s, 1H, NH); ^{13}C NMR (DMSO_d_6, ppm) 161.3 (C1), 155.1 (C2), 139.3 (C17), 128.9 (C14), 125.2 (C15), 115.6 (C16), 136.3, 133.9, 133.6, 129.2, 128.4, 127.5, 127.1, 127.0, 125.2, 124.3 (C3—C12), 21.2 (C13). Analysis (%Calculated/found) for $C_{19}H_{16}N_2O_2$ C: 75.00/75.37, H: 5.26/5.09, N: 9.21/9.12.

2.3. Synthesis of (Z)-ethyl 2-(4-(2-(1-(naphthalene-2-yl) ethylidene)hydrazinecarbonyl)-phenoxy)acetate (HL^2)

A mixture of 4-hydroxy-N′-[(1Z)-1-(aphthalene-2-yl)ethylidene]benzohydrazide (HL^1) (1 mmol, 0.304 g), ethyl bromoacetate (10 mmol, 1.670 g) and dry K_2CO_3 (10 mmol, 1.380 g) in 40 mL acetone was refluxed with stirring for 24 h and poured to 200 mL of cold water. The white precipitate formed was filtered and washed with water and finally recrystallized from ethanol.

Yield 66%; Mp 153–155 °C; UV (EtOH, nm) 272, 307sh, 366; IR (KBr) (ν, cm^{-1}) 3373 (NH), 1760 $(C{=}O)_{ester}$, 1645 $(C{=}O)_{amide}$, 1603 (C═N), 1386 (C—N), 1244 and 1077 (C—O—C); ^1H NMR (DMSO_d_6, ppm) δ 1.24 (t, J = 7.1, CH_3), 2.48 (s, 3H, N═C—CH_3), 4.17 (q, J = 7.1, OCH_2CH_3), 4.87 (s, Ar—OCH_2), 7.03 (d, 2H, J = 8.3, ArH^d), 7.23 (d, 2H, J = 8.3, ArH^e), 7.52–7.90 (m, 5H, ArH), 10.59 (s, 1H, NH); ^{13}C NMR (DMSO_d_6, ppm) 169.2 (C19), 162.0 (C1), 156.4 (C2), 138.6 (C17), 128.2 (C14), 126.0 (C15), 114.7 (C16), 136.8, 133.3, 133.7, 129.4, 128.0, 127.9, 127.3, 126.8, 125.2, 124.4 (C3—C12), 61.4 (C18), 65.3 (C20), 21.5 (C13), 14.7 (C21). Analysis (%Calculated/found) for $C_{23}H_{22}N_2O_4$ C: 70.75/71.05, H: 5.68/5.49, N: 7.17/7.42.

2.4. Synthesis of Cu(II) complexes

A solution of 1 mmol copper(II) acetate dihydrate in EtOH (10 mL) was added to a hot solution containing triethylamine (2 mmol, 0.202 g) and 2 mmol HL^1 and HL^2 in absolute ethanol (25 mL) with stirring. The reaction mixture was refluxed for 3 h. On standing over night, the complexes separated, were collected by filtration, and finally washed with water.

For $[Cu(L^1)_2]$: brown complex; yield: 83%; m.p.: 260 °C. μ_{eff} = 1.75 B.M.; UV (DMF, nm) 268, 315, 408, 432; FT-IR (KBr, cm^{-1}): 3275 b (O—H), 1605 s (C═N—N═C), 1365 (C—N), 1228 s and 1166 m (C—O—C). Analysis (%Calculated/found) for $C_{38}H_{30}CuN_4O_4$ C: 68.06/67.89, H: 4.48/4.25, N: 8.36/8.73, Cu: 9.48/9.71.

For $[Cu(L^2)_2]$: dark brown complex; yield: 80%; m.p.: 177 °C. μ_{eff} = 1.69 B.M.; UV (DMF, nm) 266, 302, 400; FT-IR (KBr, cm^{-1}): 3450 (O—H), 1758 $(C{=}{=}O)_{ester}$, 1601 (C═N—N═C), 1255 and 1167 (C—O—C). Analysis (%Calculated/found) for $C_{46}H_{44}CuN_4O_9$ C: 64.52/64.89, H: 5.11/4.95, N: 6.51/6.81, Cu: 7.56/7.23.

2.5. DNA binding

2.5.1. Electronic absorption titrations

All the experiments involving the interaction of the complexes with CT-DNA were carried out in water buffer containing 5 mM tris [tris(hydroxymethyl)aminomethane] and 50 mM NaCl, and adjusted to pH 7.3 with HCl. The solution of CT-DNA in the buffer gave a ratio of UV absorbance of 1.8–1.9:1 at 260 and 280 nm, indicating that the CT-DNA was sufficiently free of protein [26]. The CT-DNA concentration per nucleotide was determined spectrophotometrically by employing an extinction coefficient of 6600 M^{-1} cm^{-1} at 260 nm [27]. An appropriate amount of the copper complex was dissolved in a solvent mixture of 1% DMF and 99% tris–HCl buffer. Absorption titration experiments were performed by maintaining

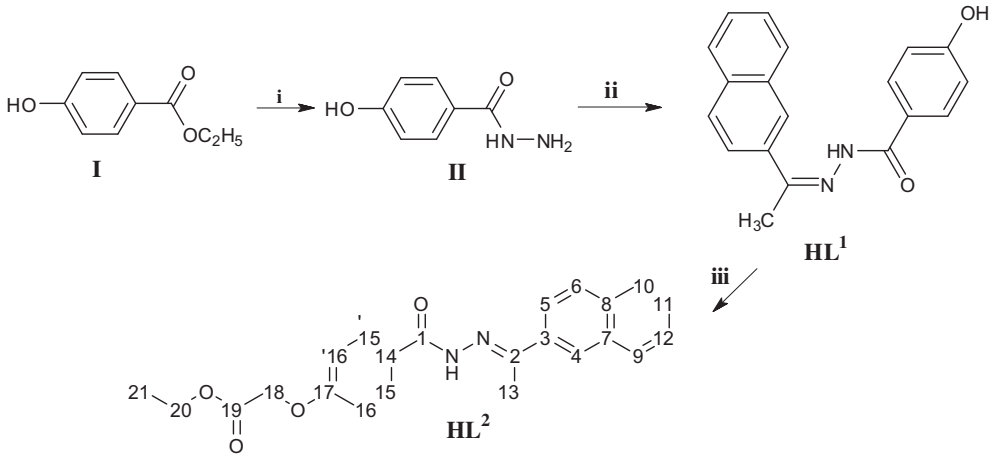

Scheme 1. Schematic diagram showing the synthesis of the acylhydrazone ligands. (i) $NH_2NH_2{\cdot}H_2O$, EtOH, reflux 4 h. (ii) methyl 2-naphthyl ketone, EtOH, AcOH, reflux 4 h; and (iii) ethyl bromoacetate, K_2CO_3, acetone, reflux 24 h.

the metal complex concentration as constant while gradually increasing the concentration of the CT-DNA within 0–100 μM.

2.6. DNA Cleavage

pBR322 plasmid DNA was used for all cleavage activities. In a typical experiment, 7 μl plasmid DNA (50 ng/μl) was mixed with different concentrations of complexes (25, 50, 75 and 100 μM dissolved in DMF) to determine optimum activation concentration. 5 μl H_2O_2 (5 mM) was added to mixture to oxidize the reactant. Finally the reaction mixture was diluted with the Tris buffer (100 mM Tris, pH: 8) to a total volume of 30 μl. After that reaction mixtures were incubated at 37 °C for 2 h. Samples (20 μl) were then incubated at 37 °C and loaded with 4 μl loading dye (0.25% bromophenol blue, 0.25% xylene cyanol, 30% glycerol, 10 mmol EDTA) on a 1% agarose gel containing 1 μg/ml of EtBr. The gel was run at 100 V for 3 h in TBE buffer and photographed under UV light. To test for the presence of reactive oxygen species generated during strand scission, reactive oxygen intermediate scavengers were added alternately to the reaction mixture. These scavengers were DMSO (100 μM), KI (100 μM), NaN_3 (100 μM) and EDTA (100 μM). Samples were treated as described above.

3. Results and discussion

Acylhydrazones such as synthesized in this work may exit in the keto or in the enol tautomeric form in the solid state (Fig. 1). The observation of strong ν(C=O) peaks for HL^1 and HL^2 in the infrared spectra of the aroylhydrazones suggests that the ligands are in the keto form in the solid state [28–30]. The tautomeric keto forms of the compounds were also indicated by observation of the amide NH and carbonyl (C=O) signals of keto forms in the ^{1}H NMR and ^{13}C NMR spectroscopies, respectively.

3.1. ^{1}H and ^{13}C NMR spectroscopy

The main ^{1}H NMR signals for each of the acylhydrazone compounds are given in the experimental section. Formation of the HL^2 was confirmed by the absence of the OH proton signal at 10.15 ppm assigned to the starting material HL^1. The D_2O exchangeable singlet resonances appeared at 10.64 and 10.59 ppm for HL^1 and HL^2 ligands are assigned to NH protons. The singlet and triplet signals observed at 4.87 ppm and at 4.17 ppm are attributed to methylene protons of $-CH_2OPh$ and $-OCH_2CH_3$ groups, respectively, in the ^{1}H NMR spectra of HL^2. The other obtained values for ^{1}H NMR chemical shifts of the acylhydrazones are given in the experimental section. These data are in agreement with those previously reported for similar compounds [28–38].

The ^{1}H NMR spectral assignments of the new acylhydrazone compound are also supported by the ^{13}C NMR spectrum. The characteristic chemical shifts of the amide carbonyl (C1) and azomethine (C2) groups of the aroylhydrazones are observed at 161.3 and 162.0 ppm and 155.1 and 156.4 ppm for HL^1 and HL^2 ligands, respectively. The signal at 169.2 ppm is assignable to the ester carbonyl group (C14) of the ligand HL^2. The chemical shifts for the carbon atoms of the aromatic rings were recorded between 114.7 and 139.3 ppm. The signals observed between 14.7 and 65.3 ppm are attributed to the aliphatic carbon atoms. These assignments are in good agreement with those previously reported for similar compounds [28–37]. These results strongly suggest that the proposed acylhydrazone compound has been formed. In the ^{1}H and ^{13}C NMR spectra of the HL^1 and HL^2 only one signal was observed for all hydrogens and carbons indicating that both acylhydrazones are the E configuration [31,32] (Fig. 2). Due to the paramagnetic nature of the copper(II) complexes, their ^{1}H and ^{13}C NMR spectra could not be obtained.

3.2. IR spectroscopy

The IR spectrum of HL^1 shows a broad O—H stretching vibration at 3290 cm^{-1}. However, in the IR spectrum of HL^2 this band disappears indicating that condensation takes place. The characteristic amide I bands are observed at 1634 and 1645 cm^{-1} for HL^1 and HL^2, respectively. On the other hand, the band observed at 1760 cm^{-1} is assigned to the ester carbonyl stretching vibration which is also characteristic for carboxylic esters. The amide NH stretching band of the HL^1 was not observed in the IR spectra probably due to overlapping with the broad OH stretching frequency. However, this band is observed clearly at 3373 cm^{-1} in IR spectra of the HL^2 ligand which is hydroxyl group free. The other characteristic IR peaks of the new compounds synthesized in this work are given in the experimental section. These values are in accord with those previously reported such compounds [28–34,37–42].

To determine the modes of the acylhydrazone ligands coordination with Cu(II) ion, we compared the IR spectra of the metal free ligands with those of the complexes. The IR spectra of the copper(II) complexes lack absorptions due to amide I [ν(C=O)], $\nu(C{=}N)_{imine}$ and ν(N—H), but show a new band between 1605 and 1601 cm^{-1} probably due to ν(C=N—N=C) stretching suggesting that the NH proton is likely lost via deprotonation induced by the metal and the resulting enolic oxygen and the azomethine nitrogen coordinate to the copper [28–34,36–39]. Therefore, from the IR spectra, it is concluded that acylhydrazones act as mono anionic bidentate ligands coordinating through the azomethine nitrogen and the enolic oxygen (Fig. 3). In the IR spectra of the copper complexes, the phenolic hydroxyl and $(C{=}O)_{ester}$ stretching vibrations are observed almost at same positions as in the metal-free ligands indicating non-participation of these groups in coordination. On the other hand, a new broad band at around 3450 cm^{-1} for $[Cu(L^2)_2]$ complex is assignable to the OH vibration of water molecule.

3.3. X-ray diffraction analysis

Single crystal XRD could not be employed to confirm the structures of the complexes since attempts to isolate crystals suitable

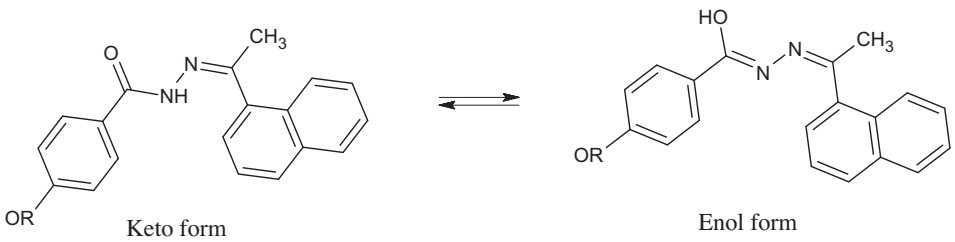

Fig. 1. Keto–enol forms of the aroylhydrazones.

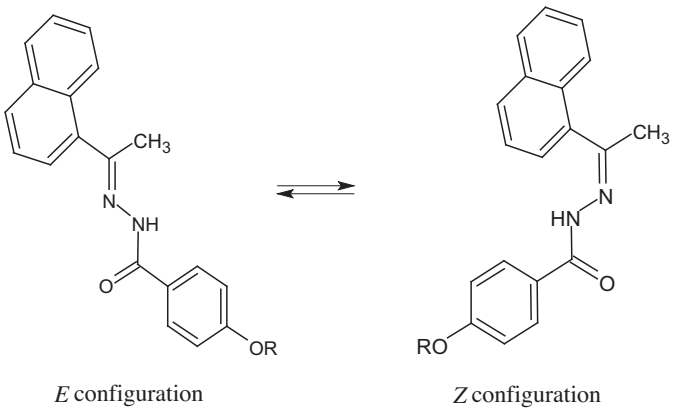

Fig. 2. Structural configurations of the acylhydrazones.

for single X-ray diffraction were unsuccessful. To obtain further evidence about the structure of the metal complexes, powder X-ray diffraction was performed (see Fig. S1). Both copper complexes show sharp crystalline peaks due to their crystalline nature. The XRD patterns for complexes are quite similar and suggest that the complexes have similar structure. The line broadening of the crystalline diffraction peaks in the $[Cu(L^1)_2]$ complexes show higher crystallinity than that of the $[Cu(L^2)_2]$ complex.

3.4. SEM and EDS analyses

The scanning electron micrographs revealed the morphology of the aroylhydrazones and their copper(II) complexes (Figs. 4 and 5). The scanning electron micrographs were taken at 15 kV accelerating voltage and magnification was fixed according to ×500. The SEM picture of the HL^1 ligand in Fig. 4a is aligned with rod-shaped blocks vertically and horizontally while its complex $[Cu(L^1)_2]$ displays agglomerated particles in non-uniform shape. The SEM image of the HL^2 (Fig. 5a) exhibits the crystalline objects are needles and rods with diagonal dimension in micrometer size. The $[Cu(L^2)_2]$ shows square shapes with irregular boundary (Fig. 5b). The average particle sizes for ligands and their Cu(II) complexes were found ~100 μm, 20 μm, 10 μm and 15 μm for HL^1, HL^2, $Cu(L^1)_2$ and $Cu(L^2)_2$, respectively. From SEM images, it is clear that there is a strong change in morphology of the hydrazone ligands after coordination to copper ion.

Energy dispersive spectroscopy (EDS) allows determining the chemical composition of a sample. Therefore, the composition of the copper complexes was defined by EDS analysis (Fig. 6). It is concluded from Fig. 6 that each complex contains only C, N, O and copper ions and existence of no other elemental peak assures the highly purity of prepared copper(II) complex powders. The EDS spectrum was appeared identical for both complexes confirming the formation of the copper complexes.

3.5. Thermal analyses

According to TGA curves, thermal degradation of $[Cu(L^1)_2]$ complex occurs in one step and it is stable under 300 °C (see Fig. S2). The degradation of this copper complex occurred within temperature range 300–480 °C corresponds the removal of the organic part of the aroylhydrazone side of the copper complexes and leaving copper oxide as a residue. On the other hand, the thermal degradation of $[Cu(L^2)_2]$ occurred in two steps. This complex showed the loss of one mole water molecule within the temperature range 185–200 °C. This high temperature loss confirms that the water molecule participate in coordination. The other step of decomposition of this complex appeared within temperature range 275–480 °C involves the removal of the organic part of ligand leaving copper oxide as a residue.

3.6. Electronic absorption spectra

The UV–Vis spectra of the aroylhydrazones and their transition metal complexes in DMF are given in the experimental section. The ligands exhibit a band around 270 nm assignable to the aromatic ring transition $\pi \rightarrow \pi^*$, which remains almost unchanged in the metal complexes. In addition, in the spectrums of the aroylhydrazones there are two transition bands at 302 and 389 for HL^1 and 307 and 366 for HL^2 corresponding to the $n \rightarrow \pi^*$ type electronic transitions. By comparison of the electronic absorption spectra of the free hydrazone ligands and their copper complexes, it is observed that the maxima bands of the free ligands showed a red shift, which may be the result of the enolization of the hydrazone ligands as well as the coordination to the copper center. The electronic spectrums of copper complexes show the metal-to-ligand charge transfer band at 432 nm and 400 nm for $[Cu(L^1)_2]$ and $[Cu(L^2)_2]$ complexes, respectively, which is comparable to those of previously reported complexes [28–34]. Unfortunately the expected weak d–d transition in the visible region for the paramagnetic copper complexes cannot be detected even with concentrated solutions. It may be lost in the low energy tail of the charge transfer transition [28–31]. The observed magnetic moment values for $[Cu(L^1)_2]$ and $[Cu(L^2)_2]$ complexes are 1.69 and 1.75 BM, respectively, which are somewhat lower and higher than the expected spin-only magnetic moment of an $S = 1/2$ (1.73 BM), Cu(II) d^9

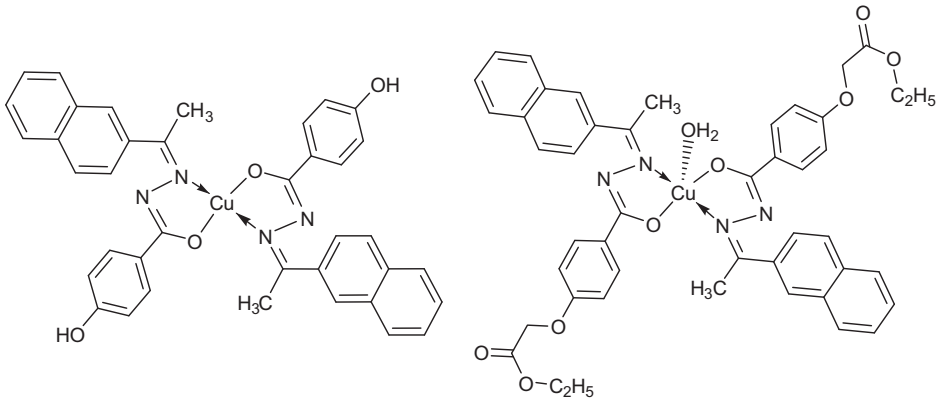

Fig. 3. Suggested structures of the copper complexes.

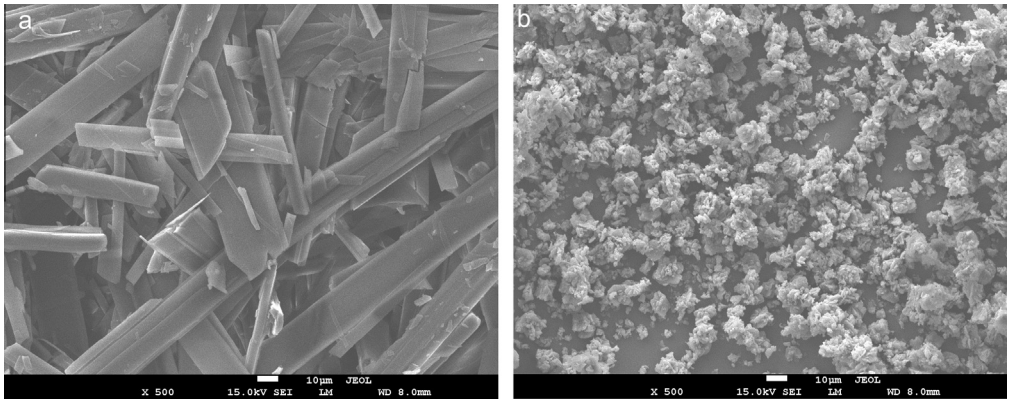

Fig. 4. SEM images of (a) HL^1 and (b) $[Cu(L^1)_2]$.

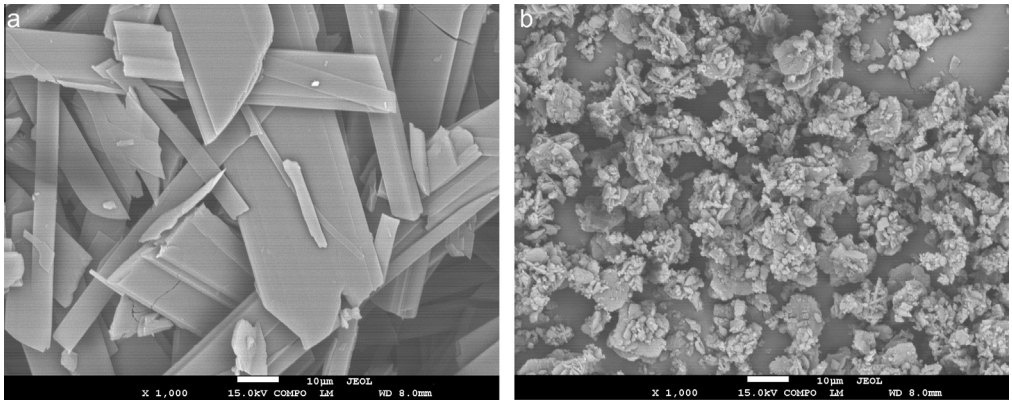

Fig. 5. SEM images of (a) HL^2 and (b) $[Cu(L^2)_2]$.

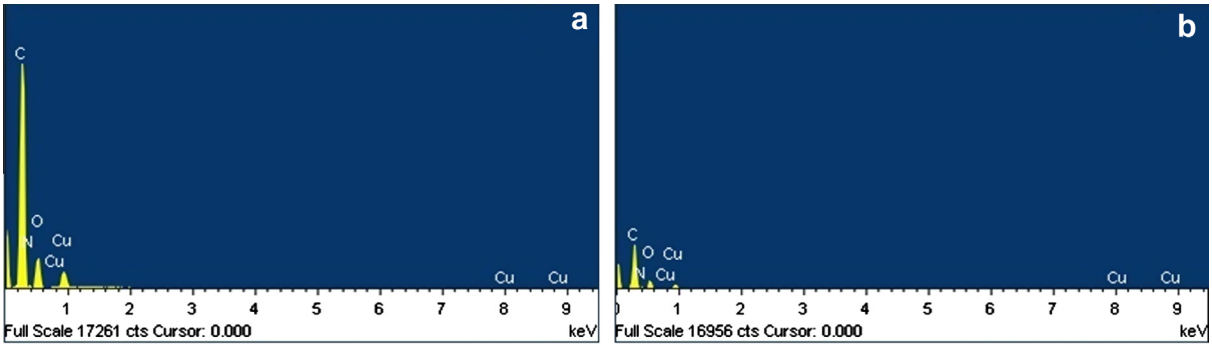

Fig. 6. Energy dispersive spectrometer of (a) $[Cu(L^1)_2]$ and (b) $[Cu(L^2)_2]$.

system, probably due to monomeric nature of the copper complexes and there is no possibility of an exchange interaction.

3.7. DNA binding studies

3.7.1. Electronic absorption titrations

It is well known that metal complexes can bind to DNA via both covalent and non-covalent interactions [43]. Non-covalent interactions include intercalation, and binding to minor groove, major groove, sugar–phosphate backbone and electrostatic binding mode [44]. Absorption titration is an effective method to examine the binding mode of DNA with metal complexes [45–47]. Drugs binding with DNA via intercalation usually result in hypochromism and bathochromism of the absorption bands due to strong stacking interactions between aromatic chromophore of molecule and the base pairs of DNA. On the other hand, the absorption intensities of drugs are increased (hyperchromism) upon increasing the concentration of CT DNA due to a damage of the CT-DNA double-helix structure. The extent of the hyperchromism is indicative of the partial or non-intercalative binding modes, such as electrostatic forces, vander Waals interaction, hydrogen bonds and hydrophobic interaction.

In the present study, the interaction of the copper complexes in DMF solutions with calf thymus DNA was investigated by the changes of absorbance at 267 nm and 314 nm for $[Cu(L^1)_2]$ (Fig. 7A) and 267 nm 304 nm for $[Cu(L^1)_2]$ with increasing concentration of CT-DNA (Fig. 7B). The spectra show clearly that the bands at 314 nm and 304 nm exhibit hypochromism of 10.13% and 9.32%

with a blue-shift of ~2 nm for the $[Cu(L^1)_2]$ and $[Cu(L^2)_2]$ complexes, respectively. On the other hand, upon addition of DNA the absorption band at 267 nm in both copper complexes is shifted to ~273 nm as well as hyperchromism of 40.85% and 31.08% in the spectra of CT-DNA/$[Cu(L^1)_2]$ and CT-DNA/$[Cu(L^2)_2]$ complexes, respectively. These changes are typical of the complexes bound to DNA through non-covalent interaction [48]. These red shifts in absorbance are accompanied by an increase in molar absorptivity, so that isosbestic points were formed at 298 nm for $[Cu(L^1)_2]$ and at 296 nm for $[Cu(L^2)_2]$ indicating the existence of single mode of binding. These spectral characteristics suggest that the binding nature of the copper complexes with DNA is similar and they might bind to DNA by an intercalative mode as well as by groove binding. The observed hypochromism could be attributed to as results of the contraction of DNA helix axes as well as the conformational changes on molecule of DNA. The two complexes in our paper interact with DNA, most likely through a mode that involves a stacking interaction between the aromatic naphthalene ring and the base pairs of DNA. On the other hand, the hyperchromism could be a result of the secondary damage of DNA double helix structure [45,49]. The carbonyl and hydroxyl groups in the copper complexes could form hydrogen bonds with suitable donors like N7 and O6 of adjacent guanine base of DNA, supported by the favorable hydrophobic interaction of naphthalene ring on the surface of DNA, contributing to the overall hyperchromism. It can be also concluded from Fig. 7 that the electronic absorption spectra of the copper complexes are not significantly changed upon addition of DNA, suggesting that the architectures of the copper complexes are not significantly modified by binding.

The intrinsic binding constant, K_b, was determined by using the equation, $[DNA]/(\varepsilon_a - \varepsilon_f) = [DNA]/(\varepsilon_o - \varepsilon_f) + 1/K_b(\varepsilon_o - \varepsilon_f)$, where [DNA] is the concentration of DNA in base pairs, ε_a, ε_f and ε_o correspond to $A_{obsd}/[M]$, the extinction coefficient of the complexes and the extinction coefficient of the complex in the fully bound form, respectively, and K_b is the intrinsic binding constant. The ratio of the slope to intercept in the plot of $[DNA]/(\varepsilon_a - \varepsilon_f)$ versus [DNA] gives the value of K_b and for complex. The calculated binding constants K_b of the copper(II) complexes $[Cu(L^1)_2]$ and $[Cu(L^2)_2]$ are 1.16×10^5 and $8.00 \times 10^4\ M^{-1}$, respectively. The results indicate that the binding strength of the $[Cu(L^1)_2]$ is stronger than that of $[Cu(L^2)_2]$, probably due to strong hydrogen bond of the hydroxyl group on the ligand of the $[Cu(L^1)_2]$ with suitable DNA nucleobases. However, the binding constants of these complexes are lower in comparison to those of the classical intercalators (for ethidium bromide and [Ru(phen)DPPZ]) [43,44].

3.8. DNA cleavage studies

The ability of the copper complexes to cleave DNA in the presence and absence of H_2O_2 was studied by gel electrophoresis using the supercoiled form of pBR322 at 37 °C in TBE buffer [21,50–53]. We prepared four different concentrations of the complexes with the range from 25 to 100 μM. The progress of the cleavage reaction with increasing concentrations of each copper complex in the

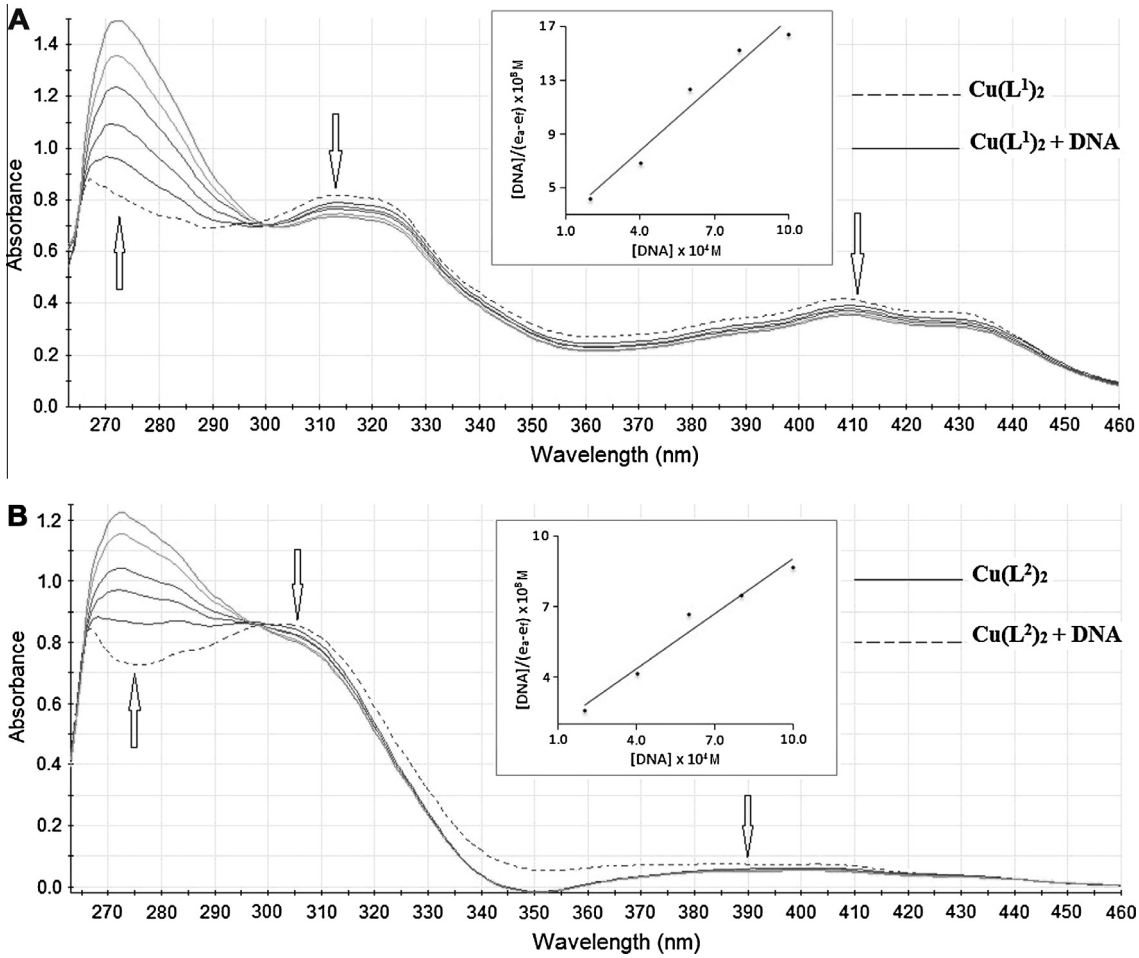

Fig. 7. Electronic spectra of Cu(II) complexes in the presence of increasing amounts of CT-DNA. [CT-DNA] = 0–100 μM. (A): $[Cu(L^1)_2]$ and (B): $[Cu(L^2)_2]$. (—) presence of T-DNA, (---) absence of CT-DNA.

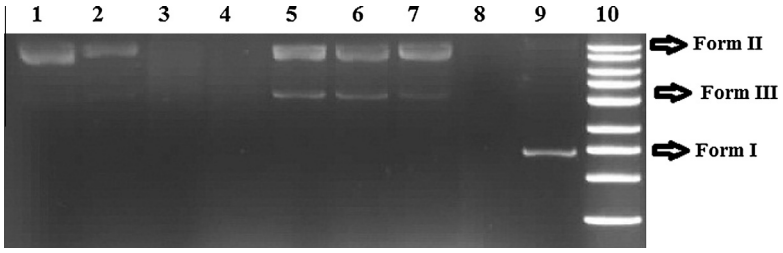

Fig. 8. Agarose gel electrophoresis of oxidative cleavage of pBR322 plasmid DNA by different concentrations of copper(II) complexes in the presence of H_2O_2. Lane 1: $Cu(L^1)_2$ (25 μM) + DNA + H_2O_2, lane 2: $Cu(L^1)_2$ (50 μM) + DNA + H_2O_2, lane 3: $Cu(L^1)_2$ (75 μM) + DNA + H_2O_2, lane 4: $Cu(L^1)_2$ (100 μM) + DNA + H_2O_2, lane 5: $Cu(L^2)_2$ (25 μM) + DNA + H_2O_2, lane 6: $Cu(L^2)_2$ (50 μM) + DNA + H_2O_2, lane 7: $Cu(L^2)_2$ (75 μM) + DNA + H_2O_2, lane 8: $Cu(L^2)_2$ (100 μM) + DNA + H_2O_2, lane 9: DNA control, lane 10: 1 kB marker.

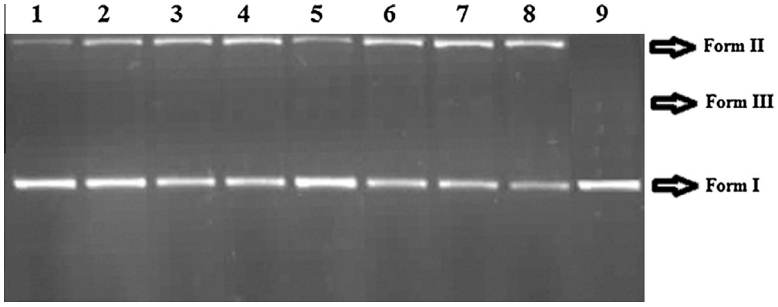

Fig. 9. Agarose gel electrophoresis of oxidative cleavage of pBR322 plasmid DNA by different concentrations of copper(II) complexes in the absence of any oxidative agent. Lane 1: $Cu(L^1)_2$ (25 μM) + DNA, lane 2: $Cu(L^1)_2$ (50 μM) + DNA, lane 3: $Cu(L^1)_2$ (75 μM) + DNA, lane 4: $Cu(L^1)_2$ (100 μM) + DNA, lane 5: $Cu(L^2)_2$ (25 μM) + DNA, lane 6: $Cu(L^2)_2$ (50 μM) + DNA, lane 7: $Cu(L^2)_2$ (75 μM) + DNA, lane 8: $Cu(L^2)_2$ (100 μM) + DNA, lane 9: DNA control.

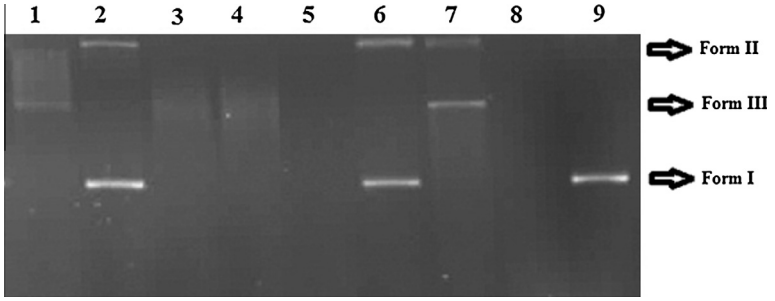

Fig. 10. Agarose gel electrophoresis of pBR322 plasmid DNA treated with the copper(II) complexes and potential inhibitors agents in the presence of hydrogen peroxide. Lane 1: $Cu(L^1)_2$ (100 μM) + DNA + H_2O_2 + NaN_3, lane 2: $Cu(L^1)_2$ (100 μM) + DNA + H_2O_2 + EDTA, lane 3: $Cu(L^1)_2$ (100 μM) + DNA + H_2O_2 + KI, lane 4: $Cu(L^1)_2$ (100 μM) + DNA + H_2O_2 + DMSO, lane 5: $Cu(L^2)_2$ (100 μM) + DNA + H_2O_2 + NaN_3, lane 6: $Cu(L^2)_2$ (100 μM) + DNA + H_2O_2 + EDTA, lane 7: $Cu(L^2)_2$ (100 μM) + DNA + H_2O + KI, lane 8: $Cu(L^2)_2$ (100 μM) + DNA + H_2O_2 + DMSO, lane 9: DNA control.

presence of H_2O_2 is given in Fig. 8. From the results shown in Fig. 8, it can be deduced that both copper complexes exhibit effective nuclease activity in the presence of hydrogen peroxide. An increase of complex concentration gives rise to an increase in the DNA cleavage. In lanes 1 and 2 for the complex $[Cu(L^1)_2]$, the circular supercoiled DNA band is completely lost and forms II and III are present. The cleavage percentage of nicked form is much higher than that of linear form. When the concentration of the $[Cu(L^1)_2]$ is increased to 75 μM, the circular supercoiled DNA degrades completely into small pieces.

With 25, 50 and 75 μM concentrations, the $[Cu(L^2)_2]$ is found to cleave the supercoiled DNA to nicked and linear DNA forms and no band is observed for form I (lanes 5–7) as a result of double-strand breaks over the plasmid molecule. It is also seen that the intensity of nicked DNA is much higher than that of form III. With increasing concentration of the copper complex, the intensity of form III also decreases. With a complex concentration of 100 μM, no band is observed, lane 8, probably due to complete degradation of DNA into small pieces.

Interestingly, both copper complexes exhibit slight nuclease activity in the absence of hydrogen peroxide as an oxidant agent. They slightly converted the form I to form II, but the supercoiled form is still seen (Fig. 9), implying that they probably undergo a mainly single-strand cleavage pathway in the absence of an oxidant agent. It is also clearly seen that as the concentration of the complex $[Cu(L^1)_2]$ increases, the concentration of the nicked DNA increases. It is reasonably expected in the absence of an oxidant agent the DNA cleavage is a hydrolytic. On the other hand, it is also reported that the DNA cleavage mediated by the some copper complexes occur via an oxidative mechanism without any reducing agent [20,21,49,53]. In this case, the oxidative DNA cleavage can be ligand-based, possibly due to the involvement of a non-diffusible organic radical mechanism which causes oxidative DNA cleavage. The other way is that the hydrogen abstraction from the deoxyribose sugar in the presence of dioxygen produces dihydrogen peroxide. Then, dihydrogen peroxide couples with Cu(II) in a Fenton-type reaction to produce reactive diffusible oxygen species, which makes the DNA cleavage oxidative

and catalytic. Further studies are undergoing to elucidate the cleavage mechanism.

3.9. Mechanism of DNA cleavage

The cleavage mechanisms of pBR322 DNA induced by $[Cu(L^1)_2]$ and $[Cu(L^2)_2]$ complexes were investigated and clarified in the presence of different scavenging agents including a hydroxyl radical scavenger (DMSO) [54,55], a hydrogen peroxide scavenger (KI) [22,56], a singlet oxygen scavenger (NaN_3) [54,56] and a chelating agent (EDTA) [54,57]. Addition of DMSO (lanes 4 and 8 in Fig. 10) does not result in any inhibition of the DNA cleavage for both complexes. This demonstrates that hydroxyl radicals are not the active oxidative species that promote the DNA cleavage by complexes. Whereas azide is ineffective for the $[Cu(L^2)_2]$ complex (lane 5), addition to DNA + $[Cu(L^1)_2]$ significantly inhibited the nuclease activity of the complex (lane 1) indicating that probably singlet oxygen radical is involved in the DNA cleavage reaction of the $[Cu(L^1)_2]$. The reason of this difference may be explained that the L^1 has a hydroxyl group which is effective in the formation of singlet oxygen in the presence of hydrogen peroxide [58]. Similarly, the significant reduction in the ability of the $[Cu(L^1)_2]$ to cleavage DNA in the presence of the KI suggests that a hydrogen peroxide-derived species is the reactive species that actually cleaves DNA. On the other hand, the hydrogen peroxide scavenger is ineffective for the $[Cu(L^1)_2]$ (lane 3). The significant reduction in the DNA cleavage abilities of the complexes in the presence of the EDTA is observed for both complexes (lanes 2 and 6), suggesting that copper ions play the key role in the cleavage.

4. Conclusions

Two new copper(II) complexes of two new Schiff base-hydrazones have been synthesized and characterized using different spectroscopic techniques. Studies on the binding of both copper complexes with DNA reflect that they can bind to CT-DNA via two binding modes: intercalation and groove binding. The $[Cu(L^1)_2]$ complex exhibits higher DNA binding affinity than that of the $[Cu(L^2)_2]$ probably because of having the —OH group of the HL^1 ligand in the copper complex, which may contribute DNA interaction by forming hydrogen bonds with suitable DNA bases. The DNA cleavage is concentration-dependent with a different pattern for both complexes in the presence of H_2O_2. The copper complex $[Cu(L^2)_2]$ cleavages the supercoiled DNA to nicked and linear DNA at the same time while, interestingly, the complex $[Cu(L^1)_2]$ can just scission form I to form II at low concentrations. On the other hand, at the high concentrations both complexes degrade the supercoiled DNA completely into small pieces. Both copper complexes show slight nuclease activity in the absence of an oxidant agent since they slightly convert the form I to form II. The mechanistic studies indicate that a hydrogen peroxide-derived species and singlet oxygen ($^1O_2$) are the active oxidative species for DNA cleavage.

Acknowledgement

We thank the Scientific Research Projects Foundation of Mugla Sıtkı Koçman University for financial support of this work.

Appendix A. Supplementary material

Supplementary data associated with this article can be found, in the online version, at http://dx.doi.org/10.1016/j.jphotobiol.2013.02.014.

References

[1] B. Rosenberg, L. VanCamp, T. Krigas, Inhibiton of cell division in escherichia coli by electrolysis products from a platinum electrode, Nature 205 (1965) 698–699.
[2] J.K. Barton, E. Lolis, Chiral discrimination in the covalent binding of bis(phenanthroline)dichlororuthenium(II) to B-DNA, J. Am. Chem. Soc. 107 (1985) 708–709.
[3] D. Charles, J.H. Turner, C. Redmond, Karyotypicprofiles of women after clomiphene citrate therapy, Bjog-Int. J. Obstet. Gee. 80 (2005) 264–271.
[4] B. Huppert (Ed.), Cisplatin, Chemistry and Biochemistry of a Heading Anticancer Drug, Wiley VCH, Weinhein, 1999.
[5] Z. Guo, P.J. Sadler, Medicinal inorganic chemistry, Adv. Inorg. Chem. 49 (2000) 183–306.
[6] K.E. Erkkila, D.T. Odom, J.K. Barton, Recognition and reaction of metallointercalators with DNA, Chem. Rev. 99 (1999) 2777–2795.
[7] B. Lippert, Multiplicity of metal ion binding patterns to nucleobases, Coord. Chem. Rev. 200 (2000) 487–516.
[8] T. Todorovic, U. Rychlewska, B. Warzajtis, D. Radanovic, N. Filipovic, I. Pajic, D. Sladic, K. Anđelkovic, Synthesis, characterization and antimicrobial activity of Ni(II) and Zn(II) complexes with N′, N′′-bis[(1E)-1-(2-pyridyl)ethylidene] propanedihydrazine. Crystal structures of two highly solvated bimetallic complexes of Ni(II), Polyhedron 28 (2009) 2397–2402.
[9] B.D. Wang, Z.Y. Yang, Q. Wang, T.K. Cai, P. Crewdson, Synthesis, characterization, cytotoxic activities, and DNA-binding properties of the La(III) complex with naringenin Schiff-base, Bioorg. Med. Chem. 14 (2006) 1880–1888.
[10] Y.Y. Karabach, A.M. Kirrillov, M. Haukka, M.N. Kopylovich, A.J.L. Pombeiro, Copper(II) coordination polymers derived from triethanolamine and pyromellitic acid for bioinspired mild peroxidative oxidation of cyclohexane, J. Inorg. Biochem. 102 (2008) 1190–1194.
[11] U. Schuchardt, W.A. Carvalho, E.V. Spinace, Why is it interesting to study cyclohexane oxidation, Syntlett 10 (1993) 713–718.
[12] A. Sigel, H. Sigel (Eds.), Metal Ions in Biological Systems, Interaction of Metal Ions with Nucleotides, Nucleic Acids, and Their Constituents, vol. 32, Marcel Dekker, New York, USA, 1996.
[13] Y. Marcus, I. Eliezer, The Stability of Mixed Complexes in Solution, Coord. Chem. Rev. 4 (1969) 273–322.
[14] M. Calvin, K.W. Wilson, Stability of chelate compounds, J. Am. Chem. Soc 67 (1945) 2003–2007.
[15] J.R.J. Sorenson, H. Sigel (Eds.), In Metal Ions in Biological Systems, Marcel Dekker, New York, 1984.
[16] R.K. Grouch, T.W. Kensler, L.W. Oberley, J.R.J. Sorenson, Biological and Inorganic Copper Chemistry, in: K.D. Karlin, J. Zubieta (Eds.), Adenine Press, Guilderland, New York, 1986.
[17] A. Yan, M.L. Tong, L.N. Ji, Z.W. Mao, Double-strand DNA cleavage by copper complexes of 2,2′-dipyridyl with electropositive pendants, Dalton Trans. 17 (2006) 2066–2071.
[18] S. Apelgot, J. Coppey, A. Fromentin, E. Guille, M.F. Poupon, A. Roussel, Altered distribution of copper (64Cu) in tumor-bearing mice and rats, Anticancer Res. 6 (1986) 159–164.
[19] P.P. Silva, W. Guerra, J.N. Silveira, A.M.C. Ferreira, T. Bortolotto, F.L. Fischer, H. Terenzi, A. Neves, E.C. Pereira-Maia, Two new ternary complexes of copper(II) with tetracycline or doxycycline and 1,10-phenanthroline and their potential as antitumoral: cytotoxicity and DNA cleavage, Inorg. Chem. 50 (2011) 6414–6424.
[20] J.T. Wang, Q. Xia, X.H. Zheng, H.Y. Chen, H. Chao, Z.W. Mao, L.N. Ji, An effective approach to artificial nucleases using copper(II) complexes bearing nucleobases, Dalton Trans. 39 (2010) 2128–2136.
[21] X.B. Yang, J. Feng, J. Zhang, Z.W. Zhang, H.H. Lin, L.H. Zhou, X.Q. Yu, Synthesis, DNA binding and cleavage activities of the copper (II) complexes of estrogen-macrocyclic polyamine conjugates, Bioorgan. Med. Chem. 16 (2008) 3871–3877.
[22] L. Jie, Z. Hao, C. Caihong, D. Hong, L. Tongbu, J. Liangnain, Interaction of macrocyclic copper (II) complexes with calf-thymus DNA: effects of the side chains of the ligands on the DNA-binding behaviors, Dalton Trans. 3 (2003) 114–119.
[23] J.K.B. Leigh, M.Z. Jeffrey, Metal complex-DNA interactions: from transcription inhibition to photoactivated cleavage, Curr. Opin. Chem. Biol. 9 (2005) 135–144.
[24] K. Dhara, J. Ratha, M. Manassero, X. Wang, S. Gao, P. Banerjee, Synthesis, crystal structure, magnetic property and oxidative DNA cleavage activity of an octanuclear copper(II) complex showing water–perchlorate helical network, J. Inorg. Biochem. 101 (2007) 95–103.
[25] I. Toyofumi, H. Hiroyuki, S. Tomoyuki, H. Masami, U. Yoshiharu, F. Yuki, Hydrolytic Cleavage of DNA by a novel copper (II) complex with cis, cis-1,3,5-triaminocyclohexane, Chem. Commun. 7 (1997) 677–678.
[26] J. Marmur, A procedure for the isolation of DNA from microorganisms, J. Mol. Biol. 3 (1961) 208–218.
[27] C.V. Kumar, E.H. Asuncion, DNA binding studies and site selective fluorescence sensitization of an anthryl probe, J. Am. Chem. Soc. 115 (1993) 8547–8553.
[28] R. Gup, B. Kırkan, Synthesis and spectroscopic studies of copper(II) and nickel(II) complexes containing hydrazonic ligands and heterocyclic coligand, Spectrochim. Acta A 62 (2005) 1188–1195.

[29] R. Gup, B. Kırkan, Synthesis and spectroscopic studies of mixed-ligand and transition metal complexes with bis-acylhydrazone tetradentate ligands and 1,10-phenanthroline, Spectrochim. Acta A 64 (2006) 809–815.
[30] R. Gup, E. Giziroğlu, Metal complexes and solvent extraction properties of isonitrosoacetophenone 2-aminobenzoylhydrazone, Spectrochim. Acta A 65 (2006) 719–726.
[31] A.A.R. Despaigne, J.G. Da Silva, A.C.M. Do Carmo, O.E. Piro, E.E. Castellano, H. Beraldo, Copper(II) and zinc(II) complexes with 2-benzoylpyridine–methyl hydrazone, J. Mol. Struct. 920 (2009) 97–102.
[32] A.P. Rebolledo, G. de Lima, L.N. Gambi, N.I. Speziali, D.F. Maia, C.B. Pinheiro, J.D. Ardisson, M.E. Cortes, H. Beraldo, Tin(IV) complexes of 2-benzoylpyridine N(4)-phenylthiosemicarbazone: spectral characterization, structural studies and antifungal activity, Appl. Organometall. Chem. 17 (2003) 945–951.
[33] S. Kulaksızoglu, C. Gokce, R. Gup, Synthesis and characterization of bis(azine) ligands and metal complexes: DNA-interaction and extraction properties for metals and dichromate anions, Turk. J. Chem. 36 (2012) 717–733.
[34] S. Naskar, S. Biswas, D. Mishra, B. Adhikary, L.R. Falvello, T. Soler, C.H. Schwalbe, S.K. Chattopadhyay, Studies on the relative stabilities of Mn(II) and Mn(III) in complexes with N_4O_2 donor environments: crystal structures of $[Mn(pybzhz)_2]$ and $[Mn(Ophsal)(imzH)_2]$ ClO_4 (pybzhz = N-(benzoyl)-N′-(picolinylidene) hydrazine, Ophsal = N, N′-o-phenylenebis(salicylideneimine), imzH = imidazole), Inorg. Chim. Acta 357 (2004) 4257–4264.
[35] R. Dinda, P. Sengupta, S. Ghash, T.C.M. Mak, Valence delocalization in a mixed-oxidation divanadium (IV, V) complex electrogenerated from Its structurally characterized divanadium (V) analogue with a tridentate (ONO) ligand, Inorg. Chem. 41 (2002) 1684–1688.
[36] A. Sreekanth, C.R. Nayar, M.R.P. Kurup, Cobalt(III) complexes of 2-hydroxyacetophenone N(4) phenyl semicarbazone containing heterocyclic coligands: syntheses, structure, and spectral studies, Polyhedron 23 (2004) 41–47.
[37] R. Dinda, P. Sengupta, S. Ghash, W.S. Sheldrick, Synthesis, structure, and reactivity of a new mononuclear molybdenum(VI) complex resembling the active center of molybdenum oxotransferases, Eur. J. Inorg. Chem. 2 (2003) 363–369.
[38] A.A.R. Despaigne, J.G. Da Silva, A.C.M. Do Carmo, F. Sives, O.E. Piro, E.E. Castellano, H. Beraldo, Copper (II) and zinc (II) complexes with 2-formylpyridine-derived hydrazones, Polyhedron 28 (2009) 3797–3803.
[39] L.L. Koh, O.L. Kon, K.W. Long, J.D. Ranford, A.L.C. Tan, Y.Y. Tjan, Complexes of salicylaldehyde acylhydrazones: cytotoxicity, QSAR and crystal structure of the sterically hindered t-butyl dimer, J. Inorg. Biochem. 72 (1998) 155–162.
[40] A.S. El-Tabl, F.A. El-Saied, W. Plass, A.N. Al-Hakimi, Synthesis, spectroscopic characterization and biological activity of the metal complexes of the Schiff base derived from phenylaminoacetohydrazide and dibenzoylmethane, Spectrochim. Acta Part A 71 (2008) 90–99.
[41] R.H. Reddy, S. Reddy, P.R. Babu, Synthesis, spectral studies and nuclease activity of mixed ligand copper(II) complexes of heteroaromatic semicarbazones/thiosemicarbazones and pyridine, J. Inorg. Biochem. 77 (1999) 169–176.
[42] S.M. Emam, S.A. AbouEl-Enein, F.A. El-Saied, S.Y. Alshater, Synthesis and characterization of some bi, tri and tetravalent transition metal complexes of N′-(furan-2-yl-methylene)-2-(p-tolylamino)acetohydrazide HL^1 and N′-(thiophen-2-yl-methylene)-2-(p-tolylamino)acetohydrazide HL^2, Spectrochim. Acta A 92 (2012) 96–104.
[43] M. Cory, D.D. McKee, J. Kagan, D.W. Henry, J.A. Miller, Design, synthesis and binding properties of bifunctional intercalators. comparison of polymethylene and diphenyl ether chains connecting phenanthridine, J. Am. Chem. Soc. 107 (1985) 2528–2536.
[44] M.J. Waring, Complex formation between ethidium bromide and nucleic acids, J. Mol. Biol. 13 (1965) 269–282.
[45] J.K. Barton, A.T. Danishhefsky, J.M. Goldberg, Tris(phenanthroline) ruthenium(II): stereoselectivity in binding to DNA, J. Am. Chem. Soc. 106 (1984) 2172–2176.
[46] J.M. Kelly, A.B. Tossi, D.J. McConnell, A study of the interactions of some polypyridylruthenium(II) complexes with DNA using fluorescence spectroscopy, topoisomerisation and thermal denaturation, Nucleic Acids Res. 13 (1985) 6017–6034.
[47] A.M. Pyle, J.P. Rehmann, J.P. Meshoyrer, C.V. Kumar, N.J. Turro, J.K. Barton, Mixed-ligand complexes of ruthenium(II): factors governing binding to DNA, J. Am. Chem. Soc. 111 (1989) 3051–3058.
[48] T. Hirohama, Y. Kuranuki, E. Ebina, T. Sugizaki, H. Arii, M. Chikira, P.T. Selvi, M. Palaniandavar, Copper(II) complexes of 1,10-phenanthroline-derived ligands: studies on DNA binding properties and nuclease activity, J. Inorg. Biochem. 99 (2005) 1205–1219.
[49] C.S. Chow, J.K. Barton, Transition metal complexes as probes of nucleic acids, Methods Enzymol. 212 (1992) 219–242.
[50] S. Banerjee, S. Mondal, S. Sen, Four new dinuclear Cu(II) hydrazone complexes using various organic spacers: syntheses, crystal structures, DNA binding and cleavage studies and selective cell inhibitory effect towards leukemic and normal lymphocytes, Dalton Trans. 46 (2009) 6849–6860.
[51] N.J. Garrido, L. Perello, R. Ortiz, Antibacterial studies, DNA oxidative cleavage, and crystal structures of Cu(II) and Co(II) complexes with two quinolone family members, ciprofloxacin and enoxacin, J. Inorg. Biochem. 99 (2005) 677–689.
[52] J.B. Lepecq, C.A. Paoletti, A fluorescent complex between ethidium bromide and nucleic acids A: physical—chemical characterization, J. Mol. Biol. 27 (1967) 87–106.
[53] P.U. Maheswari, S. Barends, S. Özalp-Yaman, P. Hoog, H. Casellas, A.J. Teat, C. Massera, M. Lutz, A.L. Spek, G.P. Wezel, P. Gamez, J. Reedijk, Unique ligand based oxidative cleavage by zinc(II) complexes of hpyramol and hpyrimol, Chem. Eur. J. 13 (2007) 5213–5222.
[54] X. Dong, X. Wang, M. Lin, H. Sun, X. Yang, Z. Guo, Promotive effect of the platinum moiety on the DNA cleavage activity of copper-based artificial nucleases, Inorg. Chem. 49 (2010) 2541–2549.
[55] B. Macias, I. Garcia, M.V. Villa, J. Borras, M.G. Alvarez, A. Castineiras, Oxidative DNA damage of mixed copper(II) complexes with sulfonamides and 1,10-phenanthroline: crystal structure of $[Cu(N\text{-quinolin-8-yl-p-toluenesulfonamidate})_2(1,10\text{-phenanthroline})]$, J. Inorg. Biochem. 96 (2003) 367–374.
[56] S.S. Massoud, F.R. Louka, W. Xu, R.S. Perkins, R. Vicente, J.H. Albering, F.A. Mautner, DNA cleavage by structurally characterized dinuclear copper(II) complexes based on triazine, Eur. J. Inorg. Chem. 23 (2011) 3469–3479.
[57] T. Ozawa, A. Hanaki, K. Onodera, Spectroscopic studies on the production of hydroxyl radicals from the reactions of copper(II)polyamine-n-polycarboxylate complexes with hydrogen peroxide, Polyhedron 11 (7) (1992) 735–738.
[58] F.A.L. Lucymara, T.A.M. Julliane, E.S. Acarızia, S.O. Ana Helena, S.T. Ana Rafaela, M.L.B. Keronninn, R.M. Glaucia, H.G.M. Mariss, D.M. Paolo, S.G. Rodrigo, F.M.M. Carlos, DNA damage by singlet oxygen and cellular protective mechanisms, Mutat. Res. – Rev. Mutat. 751 (2012) 15–28.